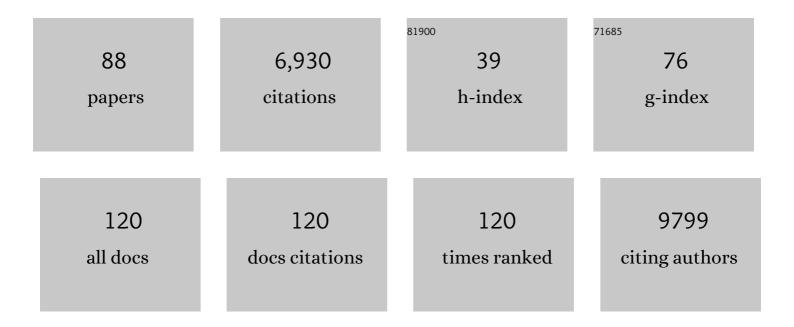
Joachim Goedhart

List of Publications by Year in descending order

Source: https://exaly.com/author-pdf/2696459/publications.pdf Version: 2024-02-01



#	Article	IF	CITATIONS
1	HI-NESS: a family of genetically encoded DNA labels based on a bacterial nucleoid-associated protein. Nucleic Acids Research, 2022, 50, e10-e10.	14.5	4
2	Single-cell imaging of ERK and Akt activation dynamics and heterogeneity induced by G-protein-coupled receptors. Journal of Cell Science, 2022, 135, .	2.0	12
3	Visualizing and Quantifying Data from Time-Lapse Imaging Experiments. Methods in Molecular Biology, 2022, 2440, 329-348.	0.9	3
4	Identification of guanine nucleotide exchange factors that increase Cdc42 activity in primary human endothelial cells. Small GTPases, 2021, 12, 226-240.	1.6	17
5	SuperPlotsOfData—a web app for the transparent display and quantitative comparison of continuous data from different conditions. Molecular Biology of the Cell, 2021, 32, 470-474.	2.1	97
6	Endothelial Focal Adhesions Are Functional Obstacles for Leukocytes During Basolateral Crawling. Frontiers in Immunology, 2021, 12, 667213.	4.8	6
7	A yeast FRET biosensor enlightens cAMP signaling. Molecular Biology of the Cell, 2021, 32, 1229-1240.	2.1	12
8	BA-plotteR – A web tool for generating Bland-Altman plots and constructing limits of agreement. Research in Veterinary Science, 2021, 137, 281-286.	1.9	12
9	Endothelial junctional membrane protrusions serve as hotspots for neutrophil transmigration. ELife, 2021, 10, .	6.0	20
10	Visualizing endogenous Rho activity with an improved localization-based, genetically encoded biosensor. Journal of Cell Science, 2021, 134, .	2.0	30
11	Imaging of Genetically Encoded FRET-Based Biosensors to Detect GPCR Activity. Methods in Molecular Biology, 2021, 2268, 159-178.	0.9	1
12	PlotXpress, a webtool for normalization and visualization of reporter expression data. F1000Research, 2021, 10, 1125.	1.6	0
13	A turquoise fluorescence lifetime-based biosensor for quantitative imaging of intracellular calcium. Nature Communications, 2021, 12, 7159.	12.8	33
14	VolcaNoseR is a web app for creating, exploring, labeling and sharing volcano plots. Scientific Reports, 2020, 10, 20560.	3.3	301
15	The cooperative action of CSB, CSA, and UVSSA target TFIIH to DNA damage-stalled RNA polymerase II. Nature Communications, 2020, 11, 2104.	12.8	91
16	High-Resolution mRNA and Secretome Atlas of Human Enteroendocrine Cells. Cell, 2020, 181, 1291-1306.e19.	28.9	110
17	PlotTwist: A web app for plotting and annotating continuous data. PLoS Biology, 2020, 18, e3000581.	5.6	53
18	Not So Dry After All: DRY Mutants of the AT1 _A Receptor and H1 Receptor Can Induce G-Protein-Dependent Signaling. ACS Omega, 2020, 5, 2648-2659.	3.5	2

2

#	Article	IF	CITATIONS
19	Sensing Extracellular Calcium – An Insight into the Structure and Function of the Calcium-Sensing Receptor (CaSR). Advances in Experimental Medicine and Biology, 2020, 1131, 1031-1063.	1.6	40
20	Physical biology of GPCR signalling dynamics inferred from fluorescence spectroscopy and imaging. Current Opinion in Structural Biology, 2019, 55, 204-211.	5.7	12
21	PlotsOfData—A web app for visualizing data together with their summaries. PLoS Biology, 2019, 17, e3000202.	5.6	443
22	In vivo characterisation of fluorescent proteins in budding yeast. Scientific Reports, 2019, 9, 2234.	3.3	71
23	Superfolder mTurquoise2 ^{ox} optimized for the bacterial periplasm allows high efficiency <i>in vivo</i> FRET of cell division antibiotic targets. Molecular Microbiology, 2019, 111, 1025-1038.	2.5	33
24	Molecular perturbation strategies to examine spatiotemporal features of Rho GEF and Rho GTPase activity in living cells. Small GTPases, 2019, 10, 178-186.	1.6	6
25	A FRET-based biosensor for measuring $\hat{Gl}\pm 13$ activation in single cells. PLoS ONE, 2018, 13, e0193705.	2.5	18
26	Optimizing FRET-FLIM Labeling Conditions to Detect Nuclear Protein Interactions at Native Expression Levels in Living Arabidopsis Roots. Frontiers in Plant Science, 2018, 9, 639.	3.6	21
27	The C-terminus of the oncoprotein TGAT is necessary for plasma membrane association and efficient RhoA-mediated signaling. BMC Cell Biology, 2018, 19, 6.	3.0	5
28	Dispense with redundant P values. Nature, 2018, 554, 31-31.	27.8	4
29	Tetraspanin microdomains control localized protein kinase C signaling in B cells. Science Signaling, 2017, 10, .	3.6	35
30	In Vivo Imaging of Diacylglycerol at the Cytoplasmic Leaflet of Plant Membranes. Plant and Cell Physiology, 2017, 58, 1196-1207.	3.1	33
31	The balance between Cα _i -Cdc42/Rac and Cα ₁ ₂ / ₁ ₃ -RhoA pathways determines endothelial barrier regulation by sphingosine-1-phosphate. Molecular Biology of the Cell, 2017, 28, 3371-3382.	2.1	57
32	Forward genetic screens identify a role for the mitochondrial HER2 in E-2-hexenal responsiveness. Plant Molecular Biology, 2017, 95, 399-409.	3.9	12
33	In vivo FRET–FLIM reveals cell-type-specific protein interactions in Arabidopsis roots. Nature, 2017, 548, 97-102.	27.8	128
34	Characterization of a spectrally diverse set of fluorescent proteins as FRET acceptors for mTurquoise2. Scientific Reports, 2017, 7, 11999.	3.3	77
35	Spatiotemporal analysis of RhoA/B/C activation in primary human endothelial cells. Scientific Reports, 2016, 6, 25502.	3.3	51
36	siFLIM: single-image frequency-domain FLIM provides fast and photon-efficient lifetime data. Nature Methods, 2016, 13, 501-504.	19.0	48

#	Article	IF	CITATIONS
37	Quantitative Single-Cell Analysis of Signaling Pathways Activated Immediately Downstream of Histamine Receptor Subtypes. Molecular Pharmacology, 2016, 90, 162-176.	2.3	23
38	Kinetics of recruitment and allosteric activation of ARHGEF25 isoforms by the heterotrimeric G-protein Gαq. Scientific Reports, 2016, 6, 36825.	3.3	19
39	F-actin-rich contractile endothelial pores prevent vascular leakage during leukocyte diapedesis through local RhoA signalling. Nature Communications, 2016, 7, 10493.	12.8	113
40	A New Generation of FRET Sensors for Robust Measurement of Gαi1, Gαi2 and Gαi3 Activation Kinetics in Single Cells. PLoS ONE, 2016, 11, e0146789.	2.5	50
41	Engineering of Optimized Fluorescent Proteins: An Overview from a Cyan and FRET Perspective. Series in Cellular and Clinical Imaging, 2015, , 3-32.	0.2	0
42	Domain analysis of the Nematostella vectensis SNAIL ortholog reveals unique nucleolar localization that depends on the zinc-finger domains. Scientific Reports, 2015, 5, 12147.	3.3	6
43	Plasma membrane restricted RhoGEF activity is sufficient for RhoA-mediated actin polymerization. Scientific Reports, 2015, 5, 14693.	3.3	81
44	<scp>SCARECROW</scp> â€ <scp>LIKE</scp> 23 and <scp>SCARECROW</scp> jointly specify endodermal cell fate but distinctly control <scp>SHORT</scp> â€ <scp>ROOT</scp> movement. Plant Journal, 2015, 84, 773-784.	5.7	52
45	Fourth-Generation Epac-Based FRET Sensors for cAMP Feature Exceptional Brightness, Photostability and Dynamic Range: Characterization of Dedicated Sensors for FLIM, for Ratiometry and with High Affinity. PLoS ONE, 2015, 10, e0122513.	2.5	230
46	A Perspective on Studying G-Protein–Coupled Receptor Signaling with Resonance Energy Transfer Biosensors in Living Organisms. Molecular Pharmacology, 2015, 88, 589-595.	2.3	28
47	A local VE-cadherin/Trio-based signaling complex stabilizes endothelial junctions through Rac1. Journal of Cell Science, 2015, 128, 3041-54.	2.0	82
48	A local VE-cadherin and Trio-based signaling complex stabilizes endothelial junctions through Rac1. Development (Cambridge), 2015, 142, e1.2-e1.2.	2.5	0
49	Development of FRET biosensors for mammalian and plant systems. Protoplasma, 2014, 251, 333-347.	2.1	31
50	<scp>SCA</scp> 14 mutation V138E leads to partly unfolded <scp>PKC</scp> γ associated with an exposed Câ€ŧerminus, altered kinetics, phosphorylation and enhanced insolubilization. Journal of Neurochemistry, 2014, 128, 741-751.	3.9	8
51	Optimization of Fluorescent Proteins. Methods in Molecular Biology, 2014, 1076, 371-417.	0.9	11
52	Effect of fixation procedures on the fluorescence lifetimes of <i>Aequorea victoria</i> derived fluorescent proteins. Journal of Microscopy, 2014, 256, 166-176.	1.8	35
53	PLCβ isoforms differ in their subcellular location and their CT-domain dependent interaction with Gαq. Cellular Signalling, 2013, 25, 255-263.	3.6	27
54	The DNAJB6 and DNAJB8 Protein Chaperones Prevent Intracellular Aggregation of Polyglutamine Peptides. Journal of Biological Chemistry, 2013, 288, 17225-17237.	3.4	122

#	Article	IF	CITATIONS
55	Signaling efficiency of Gαq through its effectors p63RhoGEF and GEFT depends on their subcellular location. Scientific Reports, 2013, 3, 2284.	3.3	14
56	Structure of a fluorescent protein from <i>Aequorea victoria</i> bearing the obligate-monomer mutation A206K. Acta Crystallographica Section F: Structural Biology Communications, 2012, 68, 878-882.	0.7	63
57	Structure-guided evolution of cyan fluorescent proteins towards a quantum yield of 93%. Nature Communications, 2012, 3, 751.	12.8	626
58	A mTurquoise-Based cAMP Sensor for Both FLIM and Ratiometric Read-Out Has Improved Dynamic Range. PLoS ONE, 2011, 6, e19170.	2.5	172
59	Real-time visualization of heterotrimeric G protein Gq activation in living cells. BMC Biology, 2011, 9, 32.	3.8	83
60	Quantitative Co-Expression of Proteins at the Single Cell Level – Application to a Multimeric FRET Sensor. PLoS ONE, 2011, 6, e27321.	2.5	59
61	Bright cyan fluorescent protein variants identified by fluorescence lifetime screening. Nature Methods, 2010, 7, 137-139.	19.0	258
62	Stochastic and reversible assembly of a multiprotein DNA repair complex ensures accurate target site recognition and efficient repair. Journal of Cell Biology, 2010, 189, 445-463.	5.2	114
63	Imaging Lipids in Living Cells. Cold Spring Harbor Protocols, 2010, 2010, pdb.top83.	0.3	17
64	Transfection of Cells with DNA Encoding a Visible Fluorescent Protein-Tagged Lipid-Binding Domain. Cold Spring Harbor Protocols, 2010, 2010, pdb.prot5457.	0.3	4
65	Practical and reliable FRET/FLIM pair of fluorescent proteins. BMC Biotechnology, 2009, 9, 24.	3.3	93
66	Imaging phosphatidylinositol 4â€phosphate dynamics in living plant cells. Plant Journal, 2009, 57, 356-372.	5.7	189
67	Chapter 5 Visible fluorescent proteins for FRET. Laboratory Techniques in Biochemistry and Molecular Biology / Edited By T S Work [and] E Work, 2009, 33, 171-223.	0.2	13
68	Fluorescence resonance energy transfer imaging of PKC signalling in living cells using genetically encoded fluorescent probes. Journal of the Royal Society Interface, 2009, 6, .	3.4	7
69	The anti-apoptotic activity associated with phosphatidylinositol transfer protein α activates the MAPK and Akt/PKB pathway. Biochimica Et Biophysica Acta - Molecular Cell Research, 2008, 1783, 1700-1706.	4.1	4
70	Quantitative Lifetime Unmixing of Multiexponentially Decaying Fluorophores Using Single-Frequency Fluorescence Lifetime Imaging Microscopy. Biophysical Journal, 2008, 95, 378-389.	0.5	48
71	PKCÎ ³ mutations in spinocerebellar ataxia type 14 affect C1 domain accessibility and kinase activity leading to aberrant MAPK signaling. Journal of Cell Science, 2008, 121, 2339-2349.	2.0	87
72	Regulation of PLCβ1a membrane anchoring by its substrate phosphatidylinositol (4,5)-bisphosphate. Journal of Cell Science, 2008, 121, 3770-3777.	2.0	18

#	Article	IF	CITATIONS
73	Dynamic in vivo interaction of DDB2 E3 ubiquitin ligase with UV-damaged DNA is independent of damage-recognition protein XPC. Journal of Cell Science, 2007, 120, 2706-2716.	2.0	95
74	Improved Green and Blue Fluorescent Proteins for Expression in Bacteria and Mammalian Cellsâ€,‡. Biochemistry, 2007, 46, 3775-3783.	2.5	132
75	Sensitive Detection of p65 Homodimers Using Red-Shifted and Fluorescent Protein-Based FRET Couples. PLoS ONE, 2007, 2, e1011.	2.5	80
76	Bright monomeric red fluorescent protein with an extended fluorescence lifetime. Nature Methods, 2007, 4, 555-557.	19.0	582
77	Cyan and Yellow Super Fluorescent Proteins with Improved Brightness, Protein Folding, and FRET FA¶rster Radius,. Biochemistry, 2006, 45, 6570-6580.	2.5	441
78	Plant G protein heterotrimers require dual lipidation motifs of Gα and Gγ and do not dissociate upon activation. Journal of Cell Science, 2006, 119, 5087-5097.	2.0	113
79	Analysis of oligonucleotide annealing by electrophoresis in agarose gels using sodium borate conductive medium. Analytical Biochemistry, 2005, 343, 186-187.	2.4	11
80	Multiparameter Imaging for the Analysis of Intracellular Signaling. ChemBioChem, 2005, 6, 1323-1330.	2.6	46
81	Sensitization of Dictyostelium chemotaxis by phosphoinositide-3-kinase-mediated self-organizing signalling patches. Journal of Cell Science, 2004, 117, 2925-2935.	2.0	95
82	Photolysis of Caged Phosphatidic Acid Induces Flagellar Excision in Chlamydomonas. Biochemistry, 2004, 43, 4263-4271.	2.5	25
83	Phospholipase D Activation Correlates with Microtubule Reorganization in Living Plant Cells[W]. Plant Cell, 2003, 15, 2666-2679.	6.6	225
84	Uniform cAMP Stimulation of Dictyostelium Cells Induces Localized Patches of Signal Transduction and Pseudopodia. Molecular Biology of the Cell, 2003, 14, 5019-5027.	2.1	98
85	Identical Accumulation and Immobilization of Sulfated and Nonsulfated Nod Factors in Host and Nonhost Root Hair Cell Walls. Molecular Plant-Microbe Interactions, 2003, 16, 884-892.	2.6	19
86	Rapid Colorimetric Quantification of Lipo-chitooligosaccharides from Mesorhizobium loti and Sinorhizobium meliloti. Molecular Plant-Microbe Interactions, 2002, 15, 859-865.	2.6	0
87	In vivofluorescence correlation microscopy (FCM) reveals accumulation and immobilization of Nod factors in root hair cell walls. Plant Journal, 2000, 21, 109-119.	5.7	61
88	Nod Factors Integrate Spontaneously in Biomembranes and Transfer Rapidly between Membranes and to Root Hairs, but Transbilayer Flip-Flop Does Not Occurâ€. Biochemistry, 1999, 38, 10898-10907.	2.5	30